

PHYSICOCHEMICAL PROBLEMS  
OF MATERIALS PROTECTION

## Corrosion Resistance Behavior of Cr–Cu Alloyed Thermo-Mechanically Treated Reinforced Bars in 3.5% NaCl Solution

Satendra Kumar<sup>a,\*</sup>, Avinash Kumar<sup>a</sup>, I. Chakradhar<sup>a</sup>, S. Manjini<sup>a</sup>, and S. L. V. P Reddy<sup>a</sup>

<sup>a</sup>Research and Development and Scientific Services, JSW Steel Ltd., Vijayanagar Works, Toranagallu, Karnataka 583275 India

\*e-mail: satmet@gmail.com

Received June 4, 2018; revised December 8, 2018; accepted December 17, 2018

**Abstract**—The corrosion resistance of reinforcing steels are of interest to the building and construction industry as it decides the durability of structures. These steels passivates under very high alkaline pore solution (leached solution from concrete). However, they corrode once they come in direct contact with chlorides ions (near sea coast and/or de-icing material) causing premature deterioration of the entire concrete structure. To protect steel bar from corrosion, they are alloyed with chromium (up to 0.50%) in steps to steel and their corrosion resistance behavior are compared with unalloyed rebar in chloride environment. In general, chromium addition in steel provides better corrosion protection through surface passivation than unalloyed one. However, in the present study, increase in chromium content in steel did not show a direct relationship to the corrosion protection of thermo mechanically treated (TMT) rebars. To ensure the corrosion protection of TMT rebars, the critical limit of chromium addition should be 0.3%. The corrosion resistance of the TMT with varying chromium content followed the following trends: TMT-0.5Cr > TMT-0.3Cr > TMT > TMT-0.1Cr.

**Keywords:** thermo mechanical treatment (TMT), corrosion, reinforcement, salt spray test, electrochemical tests

**DOI:** 10.1134/S2070205119030201

### 1. INTRODUCTION

Reinforcing bar, abbreviated as rebar, embedded in concrete provides the combined benefit of tensile and compressive strength of concrete structures. Concrete possess formability, resistance to weathering and fire, high compressive stresses however it has almost nil tensile and shear stresses. So, they are reinforced with steel rebars to overcome the ill effect of concrete. Steel rebars are the most effective material for the reinforced concrete structure due to their good strength, bonding with concrete, thermal expansion characteristics (similar to concrete), bendability and weldability qualities. The rebars are also ribbed for better bonding with concrete by means of mechanical interlocking.

To achieve long term performance of the building, the rebars strength and durability are of prime concerns for the construction industries. Durability is the ability of the structure to maintain safety and serviceability criteria during their design life. The corrosion of the rebars affects durability and service life of the structure by causing surface cracking and subsequently spalls off the concrete due to the volume expansion of the corroding steel which eventually result in premature damage of the structure and threatens the life of living things [1–5]. The life of steel reinforcement is normally better when embedded in the dense concrete. It is reported by several researchers

that the leached pore solution from the concrete is highly alkaline and promotes passivity (formation of thin protective oxide layer) over the reinforcing steel [6–8]. The passive layer provides chemical protection while the physical protection of steel rebars is through the retarding access of oxygen, moisture, and various aggressive species to the steel/concrete interface. Generally the corrosion kinetics is closely related to the rust composition and electrochemical properties. Under the corrosive environment, the  $\alpha$ -FeOOH in the rust increases whereas the  $\gamma$ -FeOOH and Fe<sub>3</sub>O<sub>4</sub> decreases resulting in the compact and adherent rust layer on the TMT steel rebars. However the breakdown of the passive film leads to the corrosion initiation and progression in presence of chloride ions [8–12]. The chloride ions can be originated either from the use of contaminated ingredients in the mix and/or from the surrounding environment in the hardened state.

Once the rebars under the concrete structure comes in contact with corrosive solution by any means, the reinforcement corrosion develops and progresses almost at a steady rate. The carbonation of concrete or penetration of harmful acidic gases into the concrete mainly occurring near industrial region is also responsible for reinforcement corrosion, is due to their tendency to reduce the pH of the concrete. The drop in pH value to an optimum level instigates the

**Table 1.** Chemical composition of TMT rebars

Nomenclature of the TMT rebars	C	Mn	S	P	Si	N	Cu	Cr
	wt %							
TMT	0.21	0.81	0.014	0.016	0.16	0.004	0.05	0.02
TMT-0.1Cr	0.14	0.73	0.008	0.080	0.15	0.004	0.35	0.12
TMT-0.3Cr	0.12	0.77	0.015	0.081	0.17	0.004	0.34	0.29
TMT-0.5Cr	0.13	0.71	0.012	0.088	0.22	0.004	0.34	0.50

reinforcement corrosion. The reinforcement corrosion depends on several other factors such as the concrete quality including water to cement ratio, cement/sand/aggregate ratio, surface cracks, if any, etc and other environmental factors like moisture, humidity, oxygen, salinity in the environment, temperature, etc. The buildup of corrosion products (iron oxides) at the rebars generates tensile stresses on the concrete from inside to outward direction leading to cracking and spalling of the concrete [13–16]. The rebars also loses interfacial bond with concrete due to the poor bonding characteristics of iron oxides with concrete. The rebars corrosion also results in reduction in cross-sectional area of the steel bar and consequently reducing the load carrying capacity of reinforced concrete structures which may further result in structure collapse, monetary loss and the loss of people. The corrosion issues of rebars are mainly associated with the structures where the concrete is exposed to salt water, as in bridges where salt is applied to roadways in winter, or in marine applications or in building near the coastal area where the humidity with chloride content is very high. Efforts have been continuously made to protect the rebar corrosion by different means such as coating on steel rebars either by organic resin or zinc coating, modifying the concrete mix or by addition of anti corrosive elements during steel making [17–20]. The coated material performs well with respect to corrosion resistance behavior even in very aggressive corrosive environment. However, the limitations of applying such coating becomes worst if the surface coating of rebars break or falls by any means. To improve the corrosion resistance of TMT rebars Nippon Steel tested high Ni and low Cu and W alloyed rebars by electrochemical methods and found that the corrosion resistance of alloyed rebars are far superior to ordinary rebars [21]. Subsequently, Nippon Steel in joint collaboration with Tata Iron and Steel Company of India developed several types of rebars containing Cu, Cr and P alloying element and found improved corrosion resistance than that of the unalloyed rebars [19, 20]. The effects of alloying element in TMT rebars on their corrosion behavior are still not understood clearly. The corrosion protection mechanism of TMT having outer martensite and inner ferrite-pearlite structure is yet to explore in detail. The present work aimed at improving the corrosion resistance of rebars

by alloying the steel with varying content of chromium which is expected to perform well during service without localized corrosion. The corrosion mechanism of varying chromium addition in TMT is studied using electrochemical impedance spectroscopy study and presented here.

## 2. EXPERIMENTAL

The TMT rebars with varying chromium content having a diameter of 12 mm were used for the present study. The chemical composition of the rebars is given in Table 1. The chromium in the TMT rebars is increased to improve their corrosion resistance due to the instantaneous formation of passive chromium oxide layer when chromium of steel rebars comes in contact with corrosive environment. The TMT rebars manufactured by steel industries in India must satisfy the requirement of Fe500 grade of IS 1786:2008. The carbon content in bars was reduced with increase in chromium to maintain their mechanical properties within the prescribed limit of the standard. The steel with the said chemical composition was manufactured through basic oxygen furnace steel making route and billets of (165 × 165) mm dimension were cast. The billets were rolled after reheating at 1050–1150°C temperature through roughing, intermediate and finishing mill to required size. TMT rebars with ribs on the surface are produced by the Tempcore process [22]. The cross section microstructure of the TMT rebars consists of harder martensite surface and softer ferrite and pearlite as a core.

### 2.1. Mechanical Testing and Metallography

Tensile testing of the rebars was performed using 250 kN Zwick tensile testing machine with video extension meter. Tensile test condition such as pre-load of 1 MPa, speed in yield range 60 MPa/s and test speed 0.008 cm/s were maintained while performing tensile test. The mechanical properties of TMT rebars are given in Table 2, which satisfy the requirements of Fe500D grade of IS 1786:2008. The micro-structural examination of TMT rebars were carried out by mounting the rebar sample using Bakelite powder in such a way that the cross section of the sample could be polished. The mounted samples were polished

**Table 2.** Mechanical properties of TMT rebars

Rebars	Yield strength, MPa	Ultimate tensile strength, MPa	Percentage elongation, %
TMT	534	632	20.5
TMT-0.1Cr	528	634	20.7
TMT-0.3Cr	529	630	20.5
TMT-0.5Cr	529	632	21.5

using various grades of emery paper as per the standard metallographic practice. Final polishing was completed with 0.1 $\mu$ m diamond paste. The polished samples were etched using 2% nital solutions followed by cleaning using ethanol. The Carl Zeiss (Model: Axiovert 40 MAT) inverted light microscope equipped with quantitative metallographic software was used for the examination of rim and core structures of TMT rebars. The photograph of the unetched cross section samples were taken for the identification of the martensite rim.

## 2.2. Corrosion Resistance Behavior of TMT Rebars with Varying Chromium Content

The corrosion resistance behavior of TMT rebars with varying chromium content from 0 to 0.5% were performed using salt spray fog testing (as per ASTM B-117 standard), potentiodynamic polarization method and electrochemical impedance spectroscopy (EIS) techniques. All the three grades of rebar having a diameter of 12 mm were taken for corrosion studies. TMT having nil chromium was also taken to understand the effect of chromium content on the corrosion resistance behavior. The details of the corrosion testing are given as under.

### 2.2.1. Electrochemical corrosion resistance testing.

The free corrosion potential measurement, potentiodynamic polarization and electrochemical impedance spectroscopy studies were performed using potentiostat/galvanostat/frequency response analyzer of AUTOLAB instrument (model: PGSTAT). Before performing the corrosion studies, the rebar samples were cut, degreased using acetone and rinsed with deionized water. The samples were hung in the beaker to dip in electrolyte solution for studies. The cross sectional area of the rebars was masked in such a way that only ribbed surface could only be exposed to the corrosive environment. The cleaned samples formed the working electrode while a silver-silver chloride (Ag–AgCl) electrode and a platinum wire served as reference and auxiliary electrodes, respectively. The working electrodes were placed in such a way that a constant area was exposed (exposed area: 10 cm<sup>2</sup>) to the electrolyte solution. Free corrosion potential (FCP) measurements were performed to understand the effect of alloying element on the potential difference in given electrolyte system. The FCP of the rebar samples were measured for half an hour till their stabiliza-

tion in the said environment. Potentiodynamic polarization tests were carried out at a scan rate of 1 mV s<sup>-1</sup> from -100 to +100 mV vs. Ag–AgCl electrode with respect to the FCP. The corrosion potential ( $E_{\text{corr}}$ ), corrosion current density ( $i_{\text{corr}}$ ), polarization resistance ( $R_p$ ) and corrosion rate were determined from the polarization curves using Tafel extrapolation method [23]. The corrosion rate can then be determined from the corrosion current density using Faraday's law [23]:

$$\text{Corrosion rate (mm/year)} = 316i_{\text{corr}}M/zF\rho.$$

Where,  $i_{\text{corr}}$  is the corrosion current density ( $\mu\text{A}/\text{cm}^2$ ),  $M$  is the molar mass of the metal (g/mol),  $z$  is the number of electrons transferred per metal atom,  $F$  is Faraday's constant and  $\rho$  is the density of the metal (g/cm<sup>3</sup>).

Electrochemical impedance spectroscopy (EIS) study was conducted by applying sinusoidal signal amplitude of 10 mV and the electrode response was analyzed in the frequency range between 10000 and 0.01 Hz in electrolyte solution at their respective FCPs. The electrolyte solution used to carry out the electrochemical test was 1% NaCl (using AR grade NaCl) with 0.04 N NaOH that have very close composition to the solution prevailing in concrete under actual condition. The polarization resistance value was measured from the Nyquist plots using electrochemical circuit fitting technique. The potentiodynamic polarization and EIS studies were repeated 4 times to ensure reproducibility of test results.

**2.2.2. Salt spray fog testing.** To understand the effect of chromium content in TMT rebars, they were subjected to the aggressive corrosive environment under salt fog condition. The rebar samples were cut to a length of 120  $\pm$  1 mm from each grade and weighed separately. The cross sectional areas of samples were coated with corrosion resistant paint (shown as photographs in Fig. 1a) so that only circumferential surface of the rebar would expose to the corrosive environment. All the samples were numbered for their identifications and hung using a nylon string at an approximate angle of 15–20° in the salt spray chamber, as shown in Fig. 1b. The samples were exposed to fog in 5% NaCl Solution for 5, 10, 15, 20, 25 and 31 days. The temperature of the salt spray chamber was maintained at approximately 35  $\pm$  1°C. Fog was collected using two fog collectors each with 80 cm<sup>2</sup> of horizontal

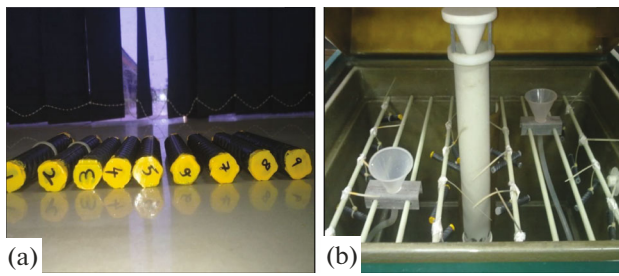


**Fig. 1.** (a) Prepared Rebar sample to be fixed in SS chamber and, (b) hanged rebars in salt spray chamber.

collecting area and maintained at a collection of 1 to 2 mL of solution per hour based on an average run of at least 16 h. After exposing the samples to salt spray atmosphere for the stipulated periods, they were removed and cleaned by dipping for 2–3 min in a solution of concentrated hydrochloric (HCl) acid with 3–5 mL of amine solution inhibitor. Amine inhibitor protects the rebar from acid corrosion during rust removal. The samples were cleaned thereafter in water flow and further dried in an oven to remove the traces of water engrossed into the pits, if any. The final mass of the tested specimen was measured for the weight loss test and the corrosion rate was determined using the following equation [23]:

$$\text{Corrosion rate (mm/year)} = (87.600 W/DAT).$$

Where  $W$  is the weight loss (g),  $D$  is the density ( $\text{g/cm}^3$ ),  $A$  is the area of exposure ( $\text{cm}^2$ ), and  $T$  is the time of exposure (h)

### 3. RESULTS

#### 3.1. Microstructure

The visual appearance of the cross section of TMT rebars is given in Fig. 2, which clearly reveals the outer rim zone and inner core of TMT rebars. To characterize the rim and core, the microstructure of one of the TMT rebar was examined using optical microscope and is shown in Fig. 3. The outer rim of the rebar clearly revealed the martensite phase whereas the core or the inner parts contain pro-eutectoid ferrite and pearlite in microstructure. Scanning electron microscopy of the rim of the rebar at higher magnification is also given in Fig. 3.

#### 3.2. Corrosion Behavior of TMT Rebars

The TMT rebars with varying chromium content were immersed for 0.5 h in electrolyte solution containing 1% NaCl with 0.04 N NaOH for stabilization and the free corrosion potential (FCP) was measured during this period. The FCP-time curves of TMT rebars are shown in Fig. 4. The FCP of all the rebars started shifting towards the active region immediately

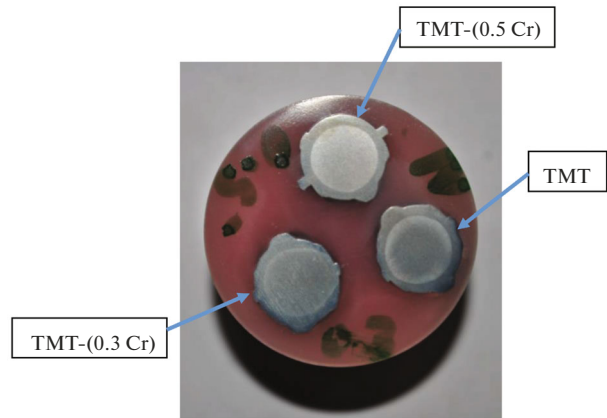


**Fig. 2.** Visual appearance of martensite rim of TMT and chromium, 0.3 and 0.5 wt % added TMT rebars.

after the interaction between electrolyte and metal which gets stabilized at their equilibrium potential. The TMT rebars with the maximum amount of chromium (0.5%) addition in present study exhibited a nobler FCP when compared with the other TMT grades of steel. The nobler FCP of TMT rebar indi-

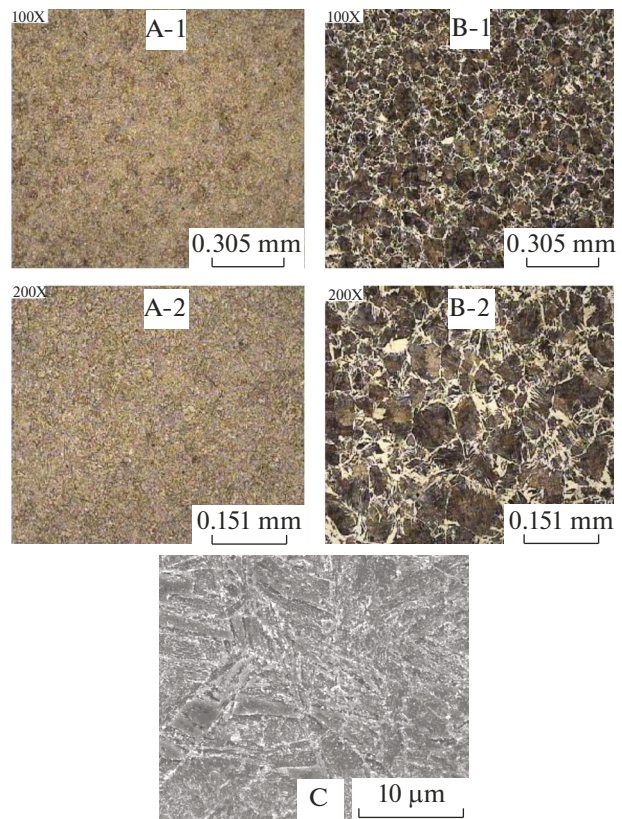


**Fig. 3.** Optical micrographs of TMT showing, (a) Tempered martensite surface, A-1: 100 $\times$ ; A-2: 200 $\times$ , (b) ferrite and pearlite at core, B-1: 100 $\times$ ; B-2: 200 $\times$ , and (c) SEM of tempered martensite at 10000 $\times$  magnification.

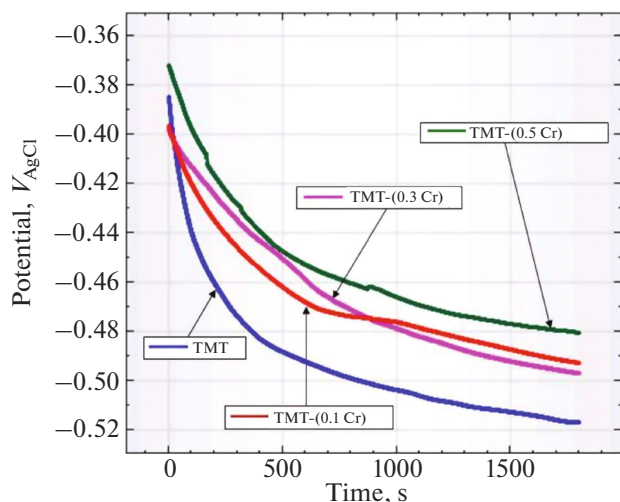


Fig. 4. Free corrosion potential with time measurement of the TMT rebars.

icates its ability to offer better corrosion protection ability. The FCP-time curve clearly revealed a positive influence of chromium addition in TMT rebar on their corrosion resistance behaviour. This is attributed due to the instantaneous passive film forming characteristics of chromium once coming in contact with corrosive environment which helps in protecting the steel from corrosion. To get a better insight about the electrochemical corrosion behavior of the TMT rebar samples, potentiodynamic polarization, electrochemical impedance and salt spray fog tests were performed.

The potentiodynamic polarization curves of TMT rebars (with varying chromium content) in electrolyte solution in the potential range of  $-100$  to  $+100$  mV vs. Ag–AgCl electrode with respect to their FCP are shown in Fig. 5a. The corrosion potential ( $E_{\text{corr}}$ ), corrosion current density ( $i_{\text{corr}}$ ) and corrosion rates of the TMT rebars are measured using Tafel extrapolation method and given in Table 3. The TMT rebar having chromium exhibits a shift in  $E_{\text{corr}}$  towards the active direction when compared to that of the TMT rebars having no chromium. However, the  $i_{\text{corr}}$  and corrosion rate of TMT rebars didn't show a regular trend with respect to increase in chromium content in it (Fig. 5b). The addition of 0.1% chromium in TMT exhibited increase in  $i_{\text{corr}}$  value which indicates its deteriorated corrosion resistance in the given electrolyte medium. Further increase in chromium from 0.1 to 0.3 and 0.5% has shown positive influence on corrosion resistance behavior. The  $i_{\text{corr}}$  and corrosion rate of TMT having 0.5%Cr exhibited the lowest value among entire rebars studied.

The Nyquist, Bode Impedance and Phase angle plots of TMT with varying chromium alloying element in electrolyte solution (containing 1% NaCl with 0.04 N NaOH) at their respective FCP, are shown in Figs. 6a–6b. The size of the semicircle of Nyquist plot does not show a trend with change in chromium in TMT rebars. The TMT without chromium in it has shown better corrosion resistance than that of the TMT having 0.1% chromium. However with increase in chromium content to 0.3 and 0.5% shows an improving trend of corrosion resistance. The EIS results are in good agreement with FCP vs time curve and the potentiodynamic polarization test results. The electrical circuit

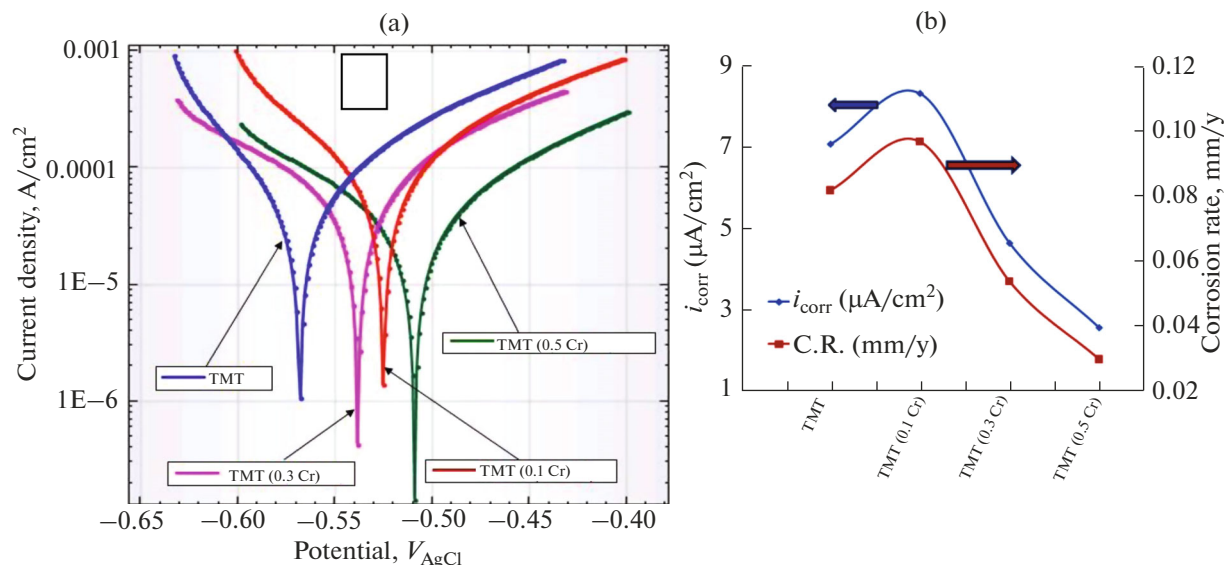


Fig. 5. (a) Potentiodynamic polarization plots of TMT rebars, (b) Variation of corrosion current density and corrosion rate with increase in chromium content in TMT; potential is scanned with respect to the Ag–AgCl reference electrode.

**Table 3.** Corrosion parameters from potentiodynamic polarization tests

Steel	Potentiodynamic polarisation test			
	$i_{\text{corr}}$ , $\mu\text{A}/\text{cm}^2$	$E_{\text{corr}}$ , mV	$R_p$ , $\Omega$	Corrosion rate, mm/y
TMT	7.1	-576	313	0.082
TMT, 0.1Cr	8.35	-534	227	0.097
TMT, 0.3Cr	4.66	-538	475	0.054
TMT, 0.5Cr	2.58	-509	796	0.030

model was also fitted and simulated with the EIS plots using BOUKAMP software to obtain the corrosion parameters, given in Table 4. The Nyquist, Bode impedance and phase angle plots of each samples with their corresponding equivalent electrical circuit model plots are presented in Figs. 7a–7d. The electrical circuit models are R[RQ] type, where the polarization resistance (R) is in parallel with the constant phase element (Q) and they are in series with the solution resistance (R). The constant phase element is similar to the capacitance where it is deviated from ideal capacitor due to the alteration of various aspects like surface defect, roughness, etc.

The corrosion resistance behavior of TMT with and without chromium alloying element is evaluated using salt spray fog test for the stipulated period of 1 month. The corrosion rates of TMT rebar steels are given in Table 5 and a graphical representation is also shown in Fig. 8. The corrosion rates after every 5 days are also examined to understand the process with increase in chromium content. The corrosion rates of TMT with and without chromium addition are in good agreement with the other test results of the present work. The corrosion resistance of 0.1% chromium addition has shown inferior corrosion resistance whereas increase in chromium from 0.1 to 0.3 and 0.5% has shown improved corrosion protection than that of the TMT without chromium addition in it. The chromium content to 0.5% in TMT has shown an excellent corrosion resistance among the other steels.

The rust layer on TMT and chromium added TMT rebars were examined using SEM coupled with EDAX

**Table 4.** The corrosion parameters obtained from EIS test after fitting and simulating the equivalent electrical circuit model

	$R_s$ , $\Omega$	$R_p$ , $\Omega$	$Y_0$ , mMho	$N$
TMT	5.50	290	35.3	0.56
TMT, 0.1Cr	6.17	180	12.2	0.50
TMT, 0.3Cr	6.14	409	4.5	0.56
TMT, 0.5Cr	6.10	447	2.2	0.62

Where  $R_s$  is the solution resistance;  $R_p$  is the polarization resistance;  $Y_0$  is the admittance;  $N$  is the exponent, if  $N = 1$ , constant phase element behave like capacitance.

to understand the influence of the alloying element of steel on rust formation. The normal TMT and 0.5% chromium added TMT are characterized for chemical constituents of rust and the microstructure of rust layers. The microstructure of rust layer are shown in Fig. 9 and their corresponding point scan for the chemical constituents present in it are given in Table 6. The corrosion products are uniform throughout which exhibits the uniform corrosion of TMT rebars without microcell formation, as it was completely immersed inside the chlorinated electrolyte solution. The corrosion behavior of metallic materials mainly depends on the surface characteristics of the material, the type of rust formed and their adherence capability under harsh aggressive environment. The rust layer of chromium added TMT rebars contains noticeable amount of chromium and copper distributed throughout the rust layer whereas no traces of chromium was observed in normal TMT rebars. The chromium and copper are strongly enriched in rust layer of TMT-CRS sample. The rust formed on chromium added TMT rebars exhibited thick and adherent than that of the normal TMT rebars and thus retard the oxygen diffusion and water penetration to the steel surface. The thinner oxide layer on normal TMT rebars is due to its poor adherence capability on the steel surface which makes it to spall off. The new and fresh surface is thus available for further corrosion and materials degradation.

As explained above, the chromium content in steel provides strong passivity, intactness of the film, compact and dense rust layer thus improving further corrosion through retardation of oxygen diffusion. The chromium alloying in steel reacts in corroding medium and forms a complex compound via partial replacement of Fe from FeOOH. Due to the solubility difference of chromium in rust and the steel, some of the chromium forms the complex compound and some are precipitated on defects and grain boundaries. Whereas copper accelerate the uniform dissolution of steel and promote early stage rust formation which helps in corrosion protection through densification of the rust, similar to chromium. The combined effect of chromium and copper as an alloying element provides intact and dense rust layer which retard oxygen diffusion and further corrosion to the substrate.

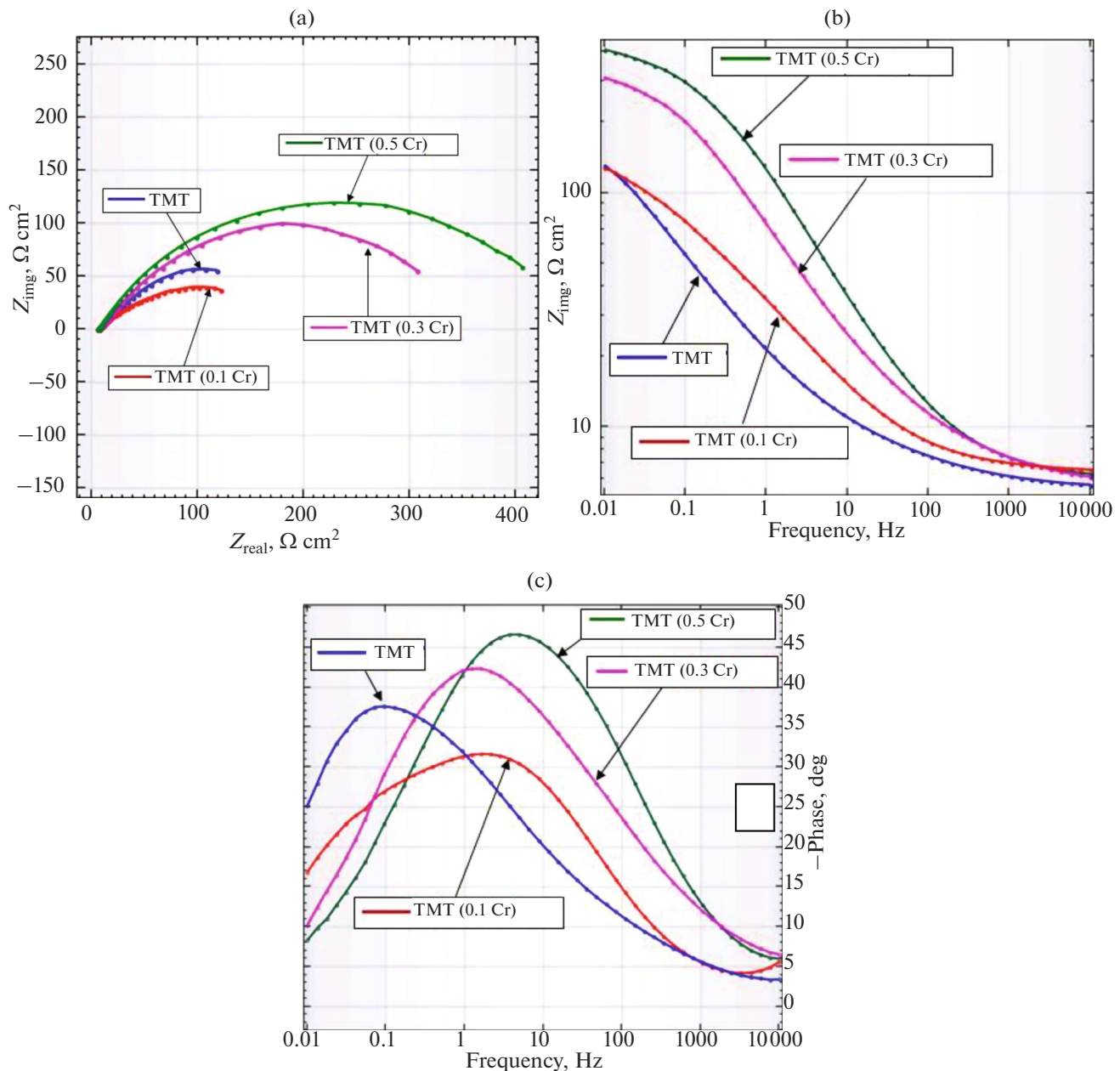


**Fig. 6.** Electrochemical impedance spectroscopy test results of TMT rebars, (a) Nyquist Plots, (b) Bode Impedance Plots and (c) Bode phase angle plots.

#### 4. DISCUSSION

The corrosion resistance behavior of TMT having 0 to 0.5% chromium content is evaluated using different corrosion testing methods and found that an optimum amount of chromium addition in steel provides better corrosion protection. The alloying of chromium in steel improves their corrosion protection ability through passive layer formation of the surface. However, only 0.1% addition of chromium in TMT rebar steel didn't show any improvement rather it deteriorates its corrosion resistance in present study. The depreciation of corrosion resistance with addition of

chromium in TMT rebars could be due to various reasons including the surface microstructure, strain, surface roughness, availability of chromium for passivation etc. The microstructure of the ribbed type outer rim of TMT rebars contains 100% martensite phase and in our previous work we observed the poor corrosion resistance of martensite than that of the ferrite and pearlite microstructure of steel [24]. The 0.1% chromium in TMT rebar may not be sufficient enough to form a passive layer on the surface having ribbed structure. The ribbed surface is also expected to increase the corrosion of rebar due to the stress con-

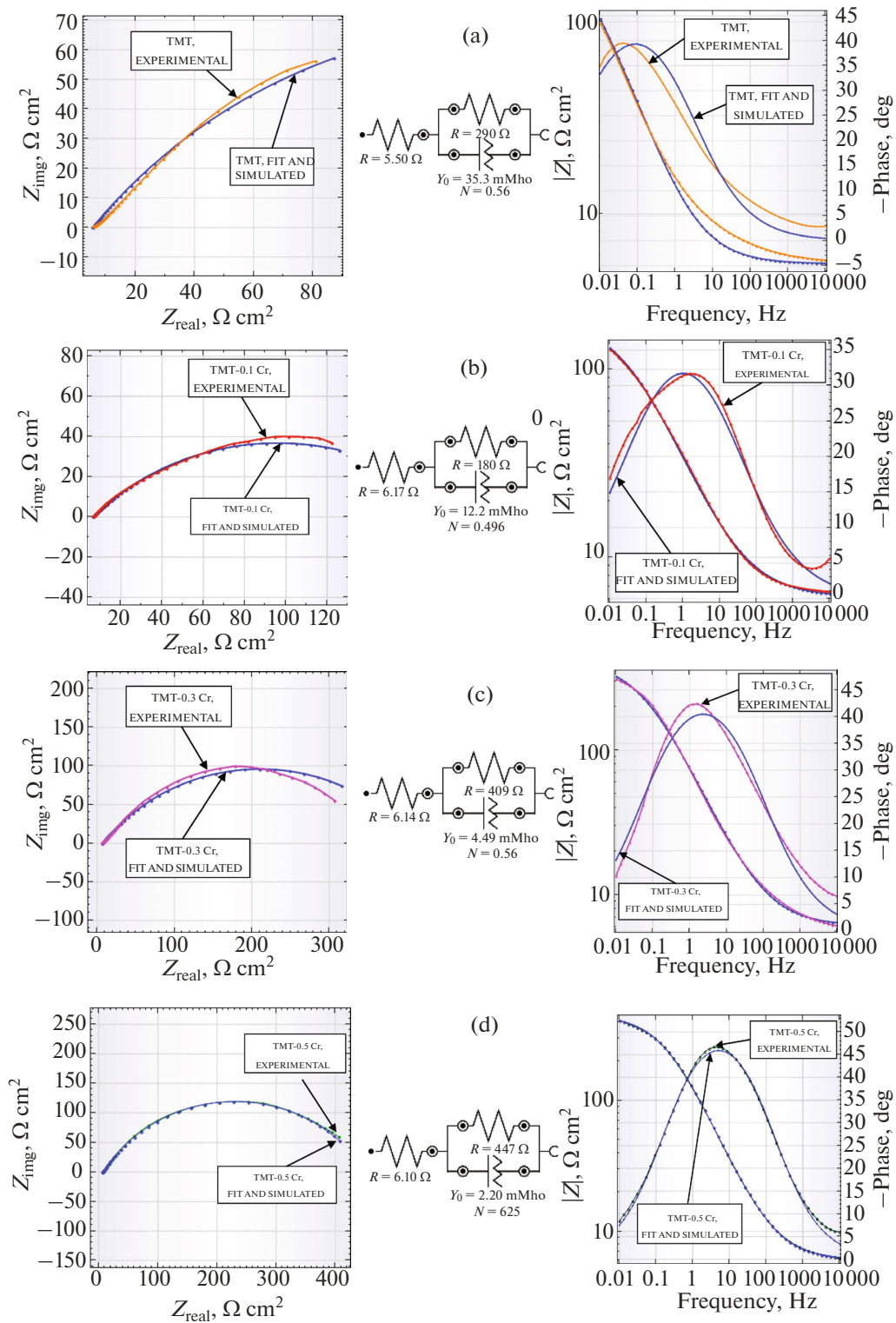


**Fig. 7.** (a–d): Non-linear least square fitting with plots obtained for the EIS data of TMT, (a) and TMT-CRS, (b) 0.1Cr, (c) 0.3Cr and, (d) 0.5Cr steel as per their equivalent electrochemical circuit models.

centration on the rib. The thinner passive layer may break in highly chlorinated electrolyte and forms micro-galvanic cell between the passive layers (chromium oxide) and pit (martensite phase of steel). The

FCP vs time curve and  $E_{\text{corr}}$  of the potentiodynamic polarization curve may be considered for the insight of the corrosion protection ability of 0.1% Cr added TMT steel. The FCP of the TMT having 0.1% Cr is in



noble state than plain TMT rebar (unalloyed with chromium) which indicates the passivity on alloyed TMT immediate after coming in contact with corrosive medium. The shift of  $E_{\text{corr}}$  to active region also confirms the instant film formation of 0.1% Cr added TMT rebars during their early stage of corrosion. The passive layers may break in the aggressive chloride environment under anodic potential application. The above said phenomena aggravate the corrosion rate due to the change in cathode to anode ratio. An increase in chromium content from 0.1 to 0.3 and 0.5% in steel provides better corrosion protection of TMT rebars as their corrosion current density are lower than the normal TMT and 0.1% Cr added TMT through intact passive layer formation.

The polarization resistance measured from the EIS plots after electrical circle fitting and simulation are also in agreement with the potentiodynamic polarisation test results. However, the mechanism of protection of TMT with varying chromium addition can well be understood from the Bode-impedance and Bode-phase angle plots. The impedance values at lowest studied frequency of Bode-impedance plots are considered as the corrosion resistance of the substrate in given electrolyte. However, the impedance at highest studied frequency is the indicative parameter of the material for its passive layer forming capability. In the present study the impedance at the highest frequency (i.e. 10.000 Hz) of all the TMT with chromium as an added alloying element exhibited higher impedance than TMT having no chromium in it. The higher impedance is an indication of better passive layer forming capability of chromium added TMT rebars. It is clearly revealed from the Bode-impedance plot (Fig. 6b) that the impedance of 0.1% chromium added TMT rebar is on the higher side at large value of frequency than plain TMT rebar which indicates an early stage protection even with small amount of chromium alloying.

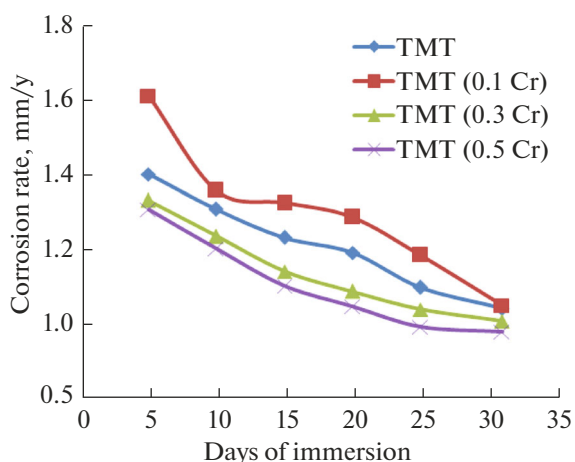


**Fig. 8.** Corrosion rate of TMT rebars at different exposure days using salt spray fog test.

**Table 5.** Corrosion rate of TMT rebars using salt spray fog tests

Days	Corrosion rate, mm/y			
	TMT	TMT-0.1Cr	TMT-0.3Cr	TMT-0.5Cr
5	1.401	1.611	1.331	1.306
10	1.307	1.357	1.235	1.201
15	1.232	1.324	1.141	1.102
20	1.191	1.287	1.088	1.047
25	1.098	1.184	1.039	0.992
31	1.042	1.050	1.007	0.979

**Table 6.** Chemical constituents of corrosion products from SEM-EDAX

TMT										
	Fe	O	Na	Mg	Al	Si	Cl	Cr	Mn	Cu
1	95.88	2.67	nd	nd	0.1	1.24	0.11	nd	nd	nd
2	83.83	10.52	0.99	nd	0.01	0.19	3.67	0.06	0.65	0.08
3	97.46	0.5	0.12	0.01	0.08	0.15	0.26	nd	0.91	0.51
4	92.62	3.05	0.38	nd	0.7	0.25	0.83	0.08	2.09	nd
TMT-0.5 Cr										
1	57.82	32.44	nd	0.13	0.07	0.21	7.56	1.02	0.14	0.61
2	72.92	24.2	0.16	nd	nd	0.16	0.41	0.79	0.6	0.76
3	59.26	36.67	0.35	nd	0	0.01	2.05	0.82	0.41	0.43
4	68.51	25.86	0.18	0.11	0.12	0.34	3.15	1.09	0.47	0.17
5	55.98	1.97	nd	nd	0.03	0.2	40.17	0.76	0.5	0.39

The impedance at lowest frequency of 0.1% chromium added TMT rebars is lower than that of plain TMT rebar indicates its inferior corrosion performance in the said electrolyte medium which corroborates the other test results. The impedance values at higher and lower frequencies provide pore solution resistance and overall polarization resistance, respectively [25]. The phase angle vs frequency (Bode phase angle) plot also revealed the similar corrosion protection mechanism of plain TMT rebars and chromium added TMT rebars. The phase angle of all the TMT rebars having

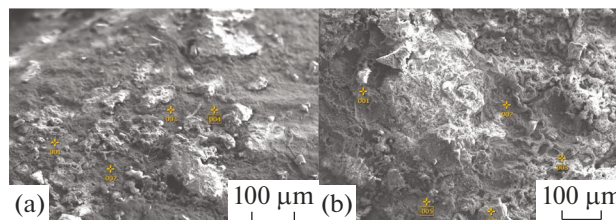


**Fig. 9.** SEM-EDAX of corrosion products of TMT and TMT-0.5Cr after salt spray fog test for 30 days duration.

chromium content achieved early phase angle peak than plain TMT rebars, indicates the early corrosion protection of material. However, the phase angle maximum of plain TMT rebars is higher than that of 0.1% chromium added TMT rebars revealing its better corrosion protection ability. The delayed phase angle maximum of plain TMT rebars is due to the poor corrosion resistance in the early stage of corrosion than that of the TMT rebars having 0.1%Cr in it. The phase angle maximum of all the TMT rebars follows the following trend TMT(0.5Cr) > TMT(0.3Cr) > TMT > TMT(0.1Cr), rebars. Salt spray fog test results also exhibited the similar corrosion resistance behavior trends. The TMT rebars having 0.3 and 0.5% chromium addition have shown better corrosion resistance property than that of the plain TMT rebars and 0.1% chromium added TMT rebars. It has also been reported elsewhere that the corrosion performance of low alloyed rebars are inferior to unalloyed rebars which supports the results presented here [26, 27]. D. Trejo and P.J. Monteiro [26] observed unexpectedly higher critical chloride threshold levels and lower corrosion rates of ordinary black reinforcing bars than low alloyed reinforcing bars embedded in concrete and chloride contaminated environment. J. Balma et al. [27] have also reported that the corrosion performance of low alloyed steel rebars are equally bad as conventional black reinforcing steel bars in chloride contaminated concrete. However, this is contradicted with the published literature showing improved corrosion resistance of rebar after alloying the steel [19, 20], hence it is worth exploring the impact of chromium with varying content (0, 0.10, 0.30 and 0.50%) in steel on corrosion resistance behavior in saline environment.

The steel substrates corrode once it comes in contact with atmospheric environment [28–30]. The most effective and economic method to improve the atmospheric corrosion resistance is addition of small amount of alloying element to develop weathering steel [31–34]. The effective alloying elements to develop weathering steel or to improve corrosion resistance behavior of steel are P, Si, Cr, Cu, Ni, Co, Al and Mo [35]. These steels exhibit significantly higher corrosion resistance than carbon steel does due to its ability in forming a compact, adherent rust layer during extended exposure [36–39]. M. Yamashita et al. [40] explained effect of chromium in weathering steel on its corrosion protection mechanism that it accumulates only in the inner rust layer leading to dense and compact layer.

The impact of chromium in improving the corrosion resistance behaviour of steel substrates can also be explained with the Pourbaix diagram, which is represented by potential versus pH diagram, providing useful information regarding regions of stability for different species of a metal [41]. P. Schmuki [42] described the Pourbaix diagram of iron in water at 25°C and explained that the corrosion of iron/steel is possible

when it is exposed to the environment with potential pH values in the region where soluble ions  $\text{Fe}^{2+}$  and  $\text{Fe}^{3+}$  is stable. Whereas, the metal exhibits passivity when exposed in the oxide formation region by forming  $\text{Fe}_3\text{O}_4$  or  $\text{Fe}_2\text{O}_3$ , and the corrosion rate is reduced tremendously. According to the Pourbaix diagram of iron, Fe is passive at higher pH. By adding Cr, the passivity region expands mostly due to the formation of a few nanometers of microcrystalline chromium oxide ( $\text{Cr}_2\text{O}_3$ ) that is protective and adherent to the passive film [43]. Y. Qian et. al. [44] have reported tremendous decrease in corrosion resistance of weathering steel when it is alloyed with 0.8% chromium in it. They concluded that the Cr content in steel from 0.8–3.0% promotes the formation of protective rust layer and decreases the corrosion rate.

The improved corrosion protection of TMT rebars in present study is attributed due to the combined effect of chromium and copper alloying element over the plain TMT rebars. The positive influence of copper in improvement in corrosion protection of steel has already been reported [45–47]. Copper in steel oxidize into Cu(I)-bearing compounds in the rust and retards its growth and oxygen supply to the steel surface, reduces the rust conductivity, retards the rust crystallization, contributes to uniform dissolution of steel and rust layer formation during initial corrosion process [45, 47, 48]. J.H. Hong et al., [49] also described the effect of copper element on corrosion retardation of steel substrate. The corrosion current density of copper containing steel was decreased due to the suppression of both the cathodic and anodic reactions. During interaction of copper containing steel with corrosive environment, preferential dissolution of the active metal than copper takes place and hence the formed rust contains both copper and iron oxide which protects the active dissolution of the steel substrate [50–55]. Y.S. Choi et al. [56] achieved significant improvement in corrosion resistance of low alloy steel alloyed with chromium, copper, calcium and nickel than the unalloyed one. They have also explained the corrosion mechanism based on the rust layer characterisation and oxides distribution in it. Under the rust layer scanning analysis using SEM–EDAX, the concentration of chromium and copper are present at the inner region of the rust confirmed their participation in protective layer formation which retards the diffusion of oxygen ion and reduces the initial corrosion. Calcium and nickel were observed at the outer region of rust layer. From the X-ray photo electron spectroscopy (XPS) analysis they found the following passive film forming compounds in rust: Cr oxides  $\text{Cr}_2\text{O}_3$ ;  $\text{Cr}(\text{OH})_3$  and  $\text{Cr}(\text{OH})\text{O}$ , copper oxides (cuprous oxide ( $\text{Cu}_2\text{O}$ ), cuprite oxide ( $\text{CuO}$ ) and cuprous chloride ( $\text{CuCl}$ )) and Ca compounds (calcium carbonate ( $\text{CaCO}_3$ ), calcium hydride ( $\text{CaH}_2$ ) and calcium oxide ( $\text{CaO}$ )). Though nickel being an alloying element to their steel, no nickel compounds was observed in the

rust layer. In present study, the copper content is increased from 0.05% of plain TMT rebars to 0.35% of TMT rebars having varied chromium content (0.1, 0.3 and 0.5%). Nickel and calcium are not added to the steel.

### CORROSION MECHANISM OF TMT REBARS

The occurrences of corrosion and its mechanism on TMT steel rebars have already been reported by several researchers and explained their behavior in simulated as well as in real conditions. The laboratory scale studies investigated the effect of various parameters like chemical constituents, heat treated TMT rebars, under aggressive electrolyte and simulated pore solution conditions, variety of surface coating, grain boundary and microstructure engineering etc. The cathodic and anodic reactions are explained as per the medium of corrosion studied. J.K. Singh and D.D. N Singh [19] explained four different stages of TMT rebars corrosion mechanism under reinforced state where they explained how the oxygen adsorbed on the surface retarding the diffusion of water and the transformation of iron to goethite and finally to magnetite. In our present study we mainly dealt with the chlorinated environment and chromium in steel and their anodic and cathodic reactions in such environments have been reported earlier [19, 57].

The corrosion products on TMT rebar would be a combination of ferrous hydroxide, ferric hydroxide, goethite, hematite/maghemite and magnetite. Chromium hydroxide would be additional compound on the corrosion product of TMT rebars having sufficient chromium content. It has also been reported by several researchers that the ferrous hydroxide forms at the initial stage of corrosion which further forms ferric hydroxide and magnetite, while ferrous chloride forms at the surface in presence of chloride content in the electrolyte medium. The ferrous hydroxide in rust dominates in absence of chloride environment. In the present study the corrosion mechanism of normal TMT differs with chromium added TMT rebars owing to the presence of chromium and copper in it. J.K. Singh and D.D.N Singh [19] have reported improvement in corrosion resistance of TMT rebars with microalloy addition of chromium and copper to 0.10 and 0.13% in steel than that compared with the unalloyed TMT rebar. The positive influence of such a small amount of chromium and copper alloy addition in steel for TMT rebars manufacturing has not been experienced by us rather our test results shows the deterioration of corrosion resistance which contradicts to their results. The difference in the corrosion test results may be due to various reasons like influence of other chemical constituents present in steel, heat treatment condition, the surface finish or the surface oxide layer, the composition of electrolyte component, adoption of materials preparation techniques etc. Owing to the above said unknown conditions one

to one comparison and their properties interpretations are not practical.

### 5. CONCLUSIONS

The TMT rebars corrosion resistance is improved with an increase in optimum quantity of chromium alloying addition in steel. Lower quantity of alloying element has shown deterioration of the corrosion resistance than that of the TMT rebars without alloying elements. The corrosion resistance of TMT rebars follow the following trend: TMT(0.5Cr) > TMT(0.3Cr) > TMT > TMT(0.1Cr). Results from different types of corrosion test experiments, 0.5% Cr added TMT rebars has shown excellent corrosion resistance among all other ones. The addition of 0.3% Cr in steel is sufficient enough to provide better corrosion resistance than unalloyed TMT rebars which indicates its passive layer forming ability in TMT rebars.

### REFERENCES

1. Duffo, G.S., Morris, W., Raspini, I., and Saragovi, C., *Corros. Sci.*, 2004, vol. 46, pp. 2143–2157.
2. Moreno, M., Morris, W., Alvarez, M.G., and Duffo, G.S., *Corros. Sci.*, 2004, vol. 46, pp. 2681–2699.
3. Garcés, P., Andrade, M.C., Saez, A., and Alonso, M.C., *Corros. Sci.*, 2005, vol. 47, pp. 289–306.
4. Lyons, R., Ing, M., and Austin, S., *Corros. Sci.*, 2005, vol. 47, pp. 413–433.
5. Gonzalez, J.A., Miranda, J.M., and Feliu, S., *Corros. Sci.*, 2004, vol. 46, pp. 2467–2485.
6. Melchers, R.E. and Li, C.Q., *ACI Mater. J.*, 2006, vol. 103, pp. 25–32.
7. Almusallam, A.A., *Constr. Build. Mater.*, 2001, vol. 15, pp. 361–368.
8. Page, C.L., Short, N.R., and Holden, W.R., *Cem. Concr. Res.*, 1986, vol. 16, pp. 79–86.
9. Elsener, B., *Cem. Concr. Compos.*, 2002, vol. 24, pp. 65–72.
10. Montemor, M.F., Simoes, A.M.P., and Ferreira, M.G.S., *Cem. Concr. Compos.*, 2003, vol. 25, pp. 491–502.
11. Andrade, C., Alonso, C., and Sarria, J., *Cem. Concr. Compos.*, 2002, vol. 24, pp. 55–64.
12. Basheer, P.A.M., Gilleece, P.R.V., Long, A.E., and McCarter, W.J., *Cem. Concr. Compos.*, 2002, vol. 24, pp. 437–449.
13. Montemor, M.F., Simoes, A.M.P., and Ferreira, M.G.S., *Cem. Concr. Compos.*, 2003, vol. 25, pp. 491–502.
14. Choi, Y.S., Kim, J.G., and Lee, K.M., *Corros. Sci.*, 2006, vol. 48, pp. 1733–1745.
15. Poupard, O., L'Hostis, V., Catinaud, S., and Petre-Lazar, I., *Cem. Concr. Res.*, 2006, vol. 36, pp. 504–520.
16. Neville, A.M. and Brooks, J.J., *Concrete Technology*, Harlow: Longman, 1990.
17. Manna, M., Naidu, G., Rani, N., and Bandyopadhyay, N., *Surf. Coat. Technol.*, 2008, vol. 202, pp. 1510–1516.

18. Han, J.S. and Park, J.H., *Corros. Sci.*, 2004, vol. 46, pp. 787–793.
19. Singh, J.K. and Singh, D.D.N., *Corros. Sci.*, 2012, vol. 56, pp. 129–142.
20. Jang, J. and Iwasaki, I., *Corrosion*, 1991, vol. 47, pp. 875–884.
21. *Salt Corrosion-Resistant Rebars, Technical Material*, Nippon Steel Corporation, 1986. Effect of Reinforcing Bar Chemical Composition on Corrosion Resistance, University of Minnesota, Center for Studies. <http://www.cts.umn.edu/Publications/ResearchReports/pdf-download.pdfid=404>.
22. Simon, P., Economopoulos, M., and Niles, P., *Iron Steel Eng.*, 1984, vol. 61, pp. 53–57.
23. Jones, D.A., *Principles and Prevention of Corrosion*, Upper Saddle River, NJ: Prentice-Hall, 1996.
24. Avinash Kumar, Satendra Kumar, Vinaya R. Madhusudhan, and Manjini, S., *Proc. CORCON 2015*, 2015, paper no. RP-05. <http://www.corcon.org/DataFiles/RP-05.pdf>.
25. Nishimura, T., *Corros. Sci.*, 2008, vol. 50, pp. 1306–1312.
26. Trejo, D. and Monteiro, P.J., *Cem. Concr. Res.*, 2005, vol. 35, pp. 562–571.
27. Balma, J., Darwin, D., Browning, J., and Locke, C., *Evaluation of Corrosion Resistance of Microalloyed Reinforcing Steel, Report no. FHWA-KS-02-9*, Kansas Department of Transportation, 2004. [http://ntl.bts.gov/lib/24000/24600/24645/KS029\\_Final\\_Rep.pdf](http://ntl.bts.gov/lib/24000/24600/24645/KS029_Final_Rep.pdf).
28. Fuente, D.D.L., Diaz, I., Simancas, J., Chico, B., and Morcillo, M., *Corros. Sci.*, 2011, vol. 53, pp. 604–617.
29. Garcia, K.E., Barrero, C.A., Morales, A.L., and Greneche, J.M., *Corros. Sci.*, 2008, vol. 50, pp. 763–772.
30. Soares, C.G., Garbatov, Y., Zayed, A., and Wang, G., *Corros. Sci.*, 2009, vol. 51, pp. 2014–2026.
31. Dong, J.H., Han, E.H., and Ke, W., *Sci. Technol. Adv. Mater.*, 2007, vol. 8, pp. 559–565.
32. Wei, F.I., *Br. Corros. J.*, 1999, vol. 26, pp. 209–214.
33. Tamura, H., *Corros. Sci.*, 2008, vol. 50, pp. 1872–1883.
34. Ma, Y.T., Li, Y., and Wang, F.H., *Corros. Sci.*, 2009, vol. 51, pp. 1725–1732.
35. Townsend, H.E., *Corrosion*, 2001, vol. 57, pp. 497–501.
36. Kamimura, T., Hara, S., and Miyuki, H., *Corros. Sci.*, 2006, vol. 48, pp. 2799–2812.
37. Natesan, M., Venkatachari, G., and Palaniswamy, N., *Corros. Sci.*, 2006, vol. 48, pp. 3584–3608.
38. Yamashita, M., Miyuki, H., and Nagano, H., *Corros. Sci.*, 1994, vol. 36, pp. 283–299.
39. Fuente, D.D.L., Diaz, I., Simancas, J., Chico, B., and Morcillo, M., *Corros. Sci.*, 2011, vol. 53, pp. 604–617.
40. Yamashita, M., Shimizu, T., Konishi, H., Mizuki, J., and Uchida, H., *Corros. Sci.*, 2003, vol. 45, pp. 381–394.
41. Pourbaix, M., *Atlas of Electrochemical Equilibria in Aqueous Solutions*, Houston, TX: NACE, 1974, p. 263.
42. Schmuki, P., *J. Solid State Electrochem.*, 2002, vol. 6, pp. 145–164.
43. Newman, R.C., *Corrosion*, 2001, vol. 57, pp. 1030–1041.
44. Qian, Y., Ma, C., Niu, D., Xu, J., and Li, M., *Corros. Sci.*, 2013, vol. 74, pp. 424–429.
45. Hao, L., Zhang, S.X., Dong, J.H., and Wei, K., *Corros. Sci.*, 2011, vol. 53, pp. 4187–4192.
46. Hao, L., Zhang, S.X., Dong, J.H., and Wei, K., *Corros. Sci.*, 2012, vol. 54, pp. 244–250.
47. Ke, W. and Dong, J.H., *Acta Metall. Sin.*, 2010, vol. 46, pp. 1365–1378.
48. Suzuki, S., Shinoda, K., Sato, M., Fujimoto, S., and Yamashita, M., *Corros. Sci.*, 2008, vol. 50, pp. 1761–1765.
49. Hong, J.H., Lee, S.H., Kim, J.G., and Yoon, J.B., *Corros. Sci.*, 2012, vol. 54, pp. 174–182.
50. Hermas, A.A., Ogura, K., and Adachi, T., *Electrochim. Acta*, 1995, vol. 40, pp. 837–844.
51. Seo, M., Hultquist, G., Leygraf, C., and Sato, N., *Corros. Sci.*, 1986, vol. 26, pp. 949–960.
52. Choi, Y.S., Shim, J.J., and Kim, J.G., *J. Alloys Compd.*, 2005, vol. 391, pp. 162–169.
53. Kim, S.T., Park, Y.S., and Kim, H.J., *Corros. Sci. Technol.*, 2002, vol. 31, pp. 122–129.
54. Kim, J.K., *Met. Mater. Int.*, 2003, vol. 9, pp. 47–51.
55. Williams, E. and Komp, F.G., *Corrosion*, 1965, vol. 21, pp. 9–16.
56. Choi, Y.S., Shim, J.J., and Kim, J.G., *J. Alloys Compd.*, 2005, vol. 391, pp. 162–169.
57. Liu, Z.G., Gao, X.H., Yu, C., Du, L.X., Li, J.P., and Hao, P.J., *Acta Metall. Sin. (Engl. Lett.)*, 2015, vol. 28, pp. 739–747.